Scattering of surface electromagnetic waves by Sn nanoparticles

Valeriy A. Sterligov[1,2], Matthias Kretschmann[3,4]

[1] *Institute of Semiconductor Physics, prosp. Nauki 41, 03028 Kiev, Ukraine*
[2] *Laboratoire de Physique de la Matière Condensée, Université de Nice, 06108 Nice Cedex 2, France*
[3] *University of California, Irvine, California 92697, USA*
[4] *Permanent address: Siemens VDO, Regensburg, Germany*

Abstract: We show numerically that the size of the nanoparticles (NPs) that scatter surface plasmon-polaritons (SPPs) is directly related to the angular position of the maximum in a scattered light distribution. Thus, the existence of one or two experimentally observed maxima in the angular distribution of the scattered light for different NP materials can be explained by a bimodal NP size distribution. We also invoke the polarization properties of the scattered light to estimate the contribution of multiple scattering processes to the observed light distribution. SPP excitation can be detected by a minimum in the reflectivity, or a maximum in the scattered light distribution. We show that this maximum exists for a wider range of NP sizes (or surface roughness) than the minimum in the reflectivity. This observation is interesting for the development of SPP based optical sensors.

OCIS codes: (240.6680) Surface plasmons; (260.3910) Optics of metals; (240.0310) Thin films.

References and links

1. U. Kreibig, M. Volmer, *Optical Properties of Metal Clusters*, (Springer-Verlag, Berlin 1995).
2. V.A. Sterligov, P. Cheyssac, R. Kofman, S.I. Lysenko, P.M. Lytvyn, B. Vohnsen, S.I. Bozhevolnyi, and A.A. Maradudin, "Near/far-field investigations of the interaction between surface waves and nanoparticles," Phys. Stat. Sol.(b) **229**, 1283 (2002).
3. P. Cheyssac, V.A. Sterligov, S.I. Lysenko, R. Kofman, "Scattering of surface plasmon-polaritons and light by metallic nanoparticles," Opt. Commun. **175**, 383 (2000).
4. T. Kume, S. Hayashi, and K. Yamamoto, "Light emission from surface plasmon polaritons mediated by metallic fine particles," Phys. Rev. B **55**, 4774 (1997).
5. A.V. Shchegrov, I.V. Novikov, and A.A. Maradudin, "Scattering of Surface Plasmon Polaritons by a Circularly Symmetric Surface Defect," Phys. Rev. Lett. **78**, 4269 (1997).
6. J.C. Stover, "*Optical Scattering: Measurement and Analysis*," (SPIE Optical Engineering Press, Bellingham, Washington 1995).
7. V.A. Sterligov, P. Cheyssac, "Appareil et procédé de caractérisation optique d'un objet," French Patent FR2832795, G01B-011/30 (2001).
8. C. Métayer, V.A. Sterligov, A. Meunier, G. Bossis, J. Persello, S.V. Svechnikov, "Field induced structures and phase separation in electrorheological and magnetorheological colloidal suspensions," J. Phys.: Cond. Matt. **16**, S3975 (2004).
9. D.S. Wiersma, M.P. van Albada, and A. Lagendijk, "Coherent Backscattering of Light from Amplifying Random Media," Phys. Rev. Lett. **75**, 1739 (1995).
10. A. Taubert, U.-M. Wiesler, and K. Müllen, "Dendrimer-controlled one-pot synthesis of gold nanoparticles with a bimodal size distribution and their self-assembly in the solid state," J. Mater. Chem. **13**(5), 1090 (2003).

1. Introduction

Optical properties of nanoparticles (NPs) have been subject of numerous studies and publications, e.g., [1-4]. Despite these studies, many questions still remain unanswered, for example how the different phases of NP materials influence the properties of surface

#7080 - $15.00 US Received 5 April 2005; revised 16 May 2005; accepted 18 May 2005

electromagnetic waves and their scattering processes. Previously obtained experimental data on SPP scattering by 8 nm Ga NPs [2, 3] shows the presence of one maximum in the angular distribution of the scattered light, while that for 6 nm Ag NPs [4] shows two maxima. However, an explanation for this behavior was not presented yet.

Another question concerns the estimation of the role of multiple scattering of SPPs and light. This is important because the distance between NPs is usually comparable to their size. To address these issues, we invoke the polarization properties of the scattered light, and analyze it for various scattering geometries.

One more important question concerns the possible applications of SPP scattering for an elaboration of sensors that detect changes of the optical properties of contacting media by measurements of a change of the parameters of SPPs excitation. Commonly in such sensors one measures the angular position of the specular reflectivity minimum. In the present paper we suggest an alternative method that is based on measurements of the angular dependence of the total integrated scatter (*TIS*). A comparison of this method with the commonly used specular reflectivity measurement promises a much better applicability.

2 Theoretical calculations

In order to analyze the angular distribution of the scattered light numerically, we employ an approach that is based on the reduced Rayleigh equation and is described in detail in [5] and the references therein. The theoretical model that is considered below assumes SPPs of the form of a plane wave scattered from a single circularly symmetric surface defect on an otherwise planar metal surface. For the latter we assume a dielectric constant ε = -15.88 appropriate for silver at a vacuum wavelength of 632.8 nm. This choice of a real valued dielectric constant implies that we neglect ohmic losses. However, such a simplification is possible since the mean free path of the SPPs in question is approximately 22 μm and much larger than the diameter of the surface defects we study numerically (<0.5 μm). We obtain the differential cross section $\sigma_{vac}(\theta, \varphi)$, measured in units of length, by dividing the power of light scattered into the vacuum region from the surface in the (θ, φ) direction by the incident power of the SPP per unit length (see Eq. (9) in Ref. [5]). Here θ is the polar angle, while φ is the azimuthal angle of scattering. For our calculations we assumed that the circularly symmetric surface defect is of Gaussian form, with the profile function $\zeta(x) = A \exp(-x^2/R^2)$. Shown in Fig. 1(a-b) are the contour plots of the differential cross section into the vacuum region for two surface defects of different sizes. Obviously, for a Gaussian protuberance with a height A = 5 nm and a width of R = 25 nm, we see that the volume waves get excited in the backward direction, while for a larger surface defect (defined by A = 50 nm and R = 250 nm), they get excited in the forward direction.

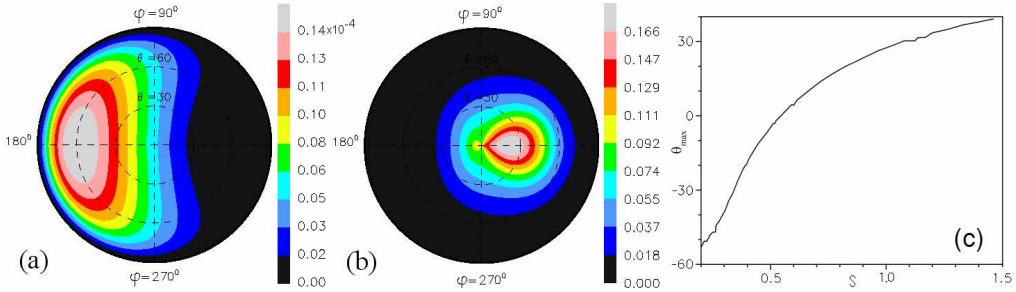

Fig. 1. The contour plots of the differential cross section (in μm) for the light scattered into the vacuum region from a Gaussian surface defect described by (a): A = 5 nm and R = 25 nm, and (b): A = 50 nm and R = 250 nm. The direction of SPPs propagation is from left to right; (c): θ_{max}, as a function of the surface defect size s.

We denote the polar angle of maximum scattering into the vacuum region as θ_{max} and plot the latter in the plane of incidence as a function of the surface defect size. We define the size s as a scalar factor such that the height of the surface defect is given as $A = s * 50$ nm, while the

#7080 - $15.00 US Received 5 April 2005; revised 16 May 2005; accepted 18 May 2005

width of the surface defect is given as $R = s * 250$ nm. From Fig. 1(c) one can see that the maximum of the differential cross section lies in the backward direction for surface defects that are smaller than $s = 0.6$, while for larger surface defects, the maximum moves towards the forward direction.

3. Experimental setup and analysis

The samples used by us were glass BK7 prisms, with a 70 nm Au film on a hypotenuse face, evaporated in UHV. This film supports the propagation of surface waves. On top of it, Sn NPs of ø8, ø16 and ø32 nm average size were evaporated and condensed. Finally, the obtained structure was protected by 3 nm film of SiO_x. For comparison, some area without NPs was incorporated onto the sample.

The normalized half-sphere distribution of scattered light, Angle Resolved Scattering (ARS) [6], was obtained by normalizing the scattered intensity I to the incident intensity Io and the solid angle dΩ of the photo detector: $ARS(\theta, \varphi) = I(\theta, \varphi)/(Io\ d\Omega)$. It was studied with a setup described in Refs. [7, 8]. In brief, the sample is placed in the first focus of an elliptical mirror that covers the whole half sphere above the sample and reflects all scattered light in the direction of a CCD camera which is placed in the second focus of the same mirror and aligned in a way that enables one to write the half sphere distribution of scattered light intensity. The polarizer in the incident beam and the analyzer in front of the CCD camera enables to control the polarization state of the analyzed light. We use the XY notation to indicate its polarization state: X denotes the polarization of the incident beam (X = S or P), while Y (Y = N, S or P) indicates the absence of an analyzer (N) or its corresponding position (S or P). Within the experimental setup it is possible to vary the angle of incidence of the beam i to record the $I(\theta, \varphi, i)$ dependence.

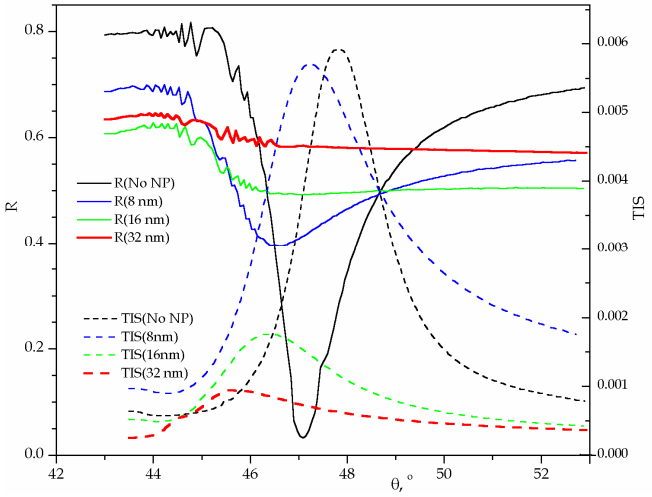

Fig. 2. Angular dependence of Rp and TIS for a zone without NPs and zones with different NP sizes.

The dependencies of the specular reflectivity for *P* polarization (*Rp*) and the *TIS* versus *i* for different sample zones with NP size *d* are presented in Fig. 2. For a zone without NPs, the minimum of *Rp* (R_{min}) that corresponds to the angle of optimal SPP excitation (i_{min}) is deeper and narrower than that for the zones with NPs. We observe that increasing *d* increased the half width of the minimum and decreased the R_{min} value. However, for $d > 8$ nm, the minimum of the $Rp(i, d)$ dependence disappears. A weak interference structure of $Rp(i, d)$ near 45° is due to interference effects with the beam that is reflected from the leg face of the prism.

In Fig. 2 the data of $TIS(i, d)$ for different zones is presented for comparison. These dependencies are characterized by the presence of a well-pronounced maximum. As *d* increases, the angular position of this maximum i_{max} shifts to smaller *i*, and its half-width

#7080 - $15.00 US
Received 5 April 2005; revised 16 May 2005; accepted 18 May 2005

increases. A comparison of *TIS*(*i*, *d*) with the *Rp*(*i*, *d*) dependencies reveals the fact that the range of *d* values for which the maximum of *TIS*(*i*, *d*) exists is much larger than the corresponding range for *Rp*(*i*, *d*). The extended range of *d* values for which a well-visible maximum of *TIS*(*i*, *d*) exists is an additional reason for choosing this investigative tool for our further studies of SPP excitation.

The *ARS*(*θ, φ*) dependencies for different polarization states of incident and scattered light are presented in Fig. 3. The shape of the *ARS*(*θ, φ, PN*) dependence in Fig. 3(a) is rather complicated. However, an analysis of the polarization of the scattered light provides important information about its essential components: the *ARS*(*θ, φ, PP*) distribution clearly shows the presence of two maxima, one in the forward and one in the backward direction relative to that of the direction of propagation of the SPP. For orthogonal polarization, *ARS*(*θ, φ, PS*) shows a well-pronounced minimum along the plane of incidence; out of this plane, the magnitude of *ARS*(*θ, φ, PS*) significantly increases and becomes comparable to that of *ARS*(*θ, φ, PP*). *ARS*(*θ, φ, SP*) is characterized by a significantly lower value of scattered intensity and the presence of a unique maximum in the forward direction. This dependence reflects the space distribution of light scattered without SPP excitation, because of the *S* polarization of the incident beam.

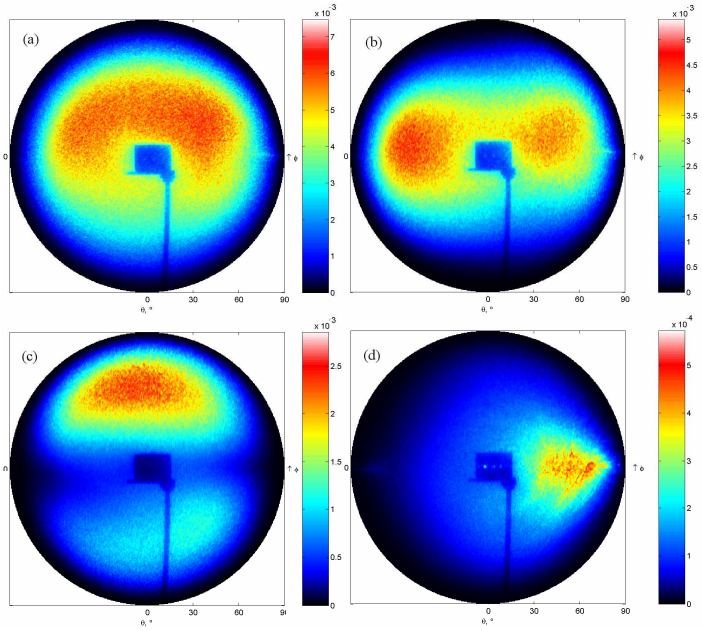

Fig. 3. The polarization properties of ARS(θ, φ) for ø8 nm Sn NP: (a) – PN, (b) – PP, (c) – PS, (d) – SP. The direction of SPP propagation is from left to right. The angle of incidence i = 46.17°. Anisotropy of ARS(θ, φ, XY) relative to the horizontal axis is probably related to some error in the prism shape.

The possible role of Coherent Backscattering (CBS) was analyzed with a traditional experiment of such kin d [9]. After a careful examination of the obtained angular distribution of the scattered light, we did not find the presence of a backscattering cone, at least in the backward direction: $I_m/I_1 - 1 < 3\%$, where I_1 and I_m are the beam intensities for single and multiple scattering, respectively.

Figure 4 and the corresponding video-recording illustrate variations of the half-sphere distribution of the SPPs scattered intensity as a function of the angle of incidence *i*. The range of i ($43^o < i < 53^o$) was chosen, so that the maximum of SPP excitation is inside it. These values are suggested by the results presented in Fig. 1, even though, strictly speaking our calculations dealt with the reciprocal process. The experimental data for the SPP scattering shows the presence of forward and backward maxima in the half-sphere light distribution. The

#7080 - $15.00 US Received 5 April 2005; revised 16 May 2005; accepted 18 May 2005

variations of the shape and amplitude of these maxima with the angle of incidence are different.

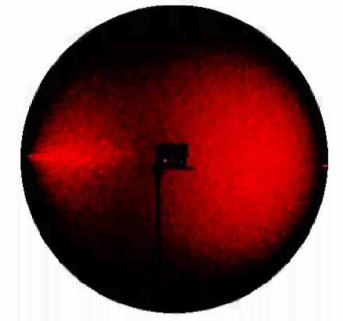

Fig. 4. Video-recording (1.5 Mb) of the dependence of $I(\theta, \varphi, \imath)$ with PP polarization on the angle of incidence (i = 43º-53º) for Ø16 nm Sn NPs. The direction of SPP propagation is from right to left.

4. Discussion of results

A change of the NPs' size can be regarded as a change of effective surface roughness. A comparison of the *TIS* and *Rp* data presented in Fig. 2 shows that the range of NPs sizes, i.e. the effective surface roughness for which a minimum of $Rp(i)$ exists is much smaller than the range for which the $TIS(i)$ maximum exists, while the angular half-widths of these dependences are comparable in the ranges of existence. This observation demonstrates a very important application possibility of the scattered light measurement for developments of different surface optical sensors that use SPPs excitation.

A tentative explanation may be related to the local nature of scattering produced by the well-localized space position of the NP film, while the $R(i)$ minimum is some integral characteristic of the SPPs excitation. SPP excitation and the corresponding transfer of incident light energy to surface waves produce a well-pronounced minimum in the $Rp(i)$ dependence, i_{min}, see Fig. 2. Its angular position depends on the whole set of SPP excitation characteristics: SPP dispersion, absorption, scattering, etc. If one does not take into account surface roughness, an ensemble of NPs is well localized in a unique definite plane, and thus the SPPs contribution to the scattered energy is related only to the local intensity of the electromagnetic field in this plane. The value of i_{max} indicates the angle of incidence that corresponds to the maximum of the electromagnetic field in the plane of the NP locations. This is the reason for the small but noticeable difference between i_{min} and i_{max}.

As was noted in the introduction, there are big differences between the $ARS(\theta, \varphi)$ dependencies for different metal NPs of comparable sizes. From a theoretical point of view, we believe that a small change in the dielectric function, caused, for example, by the phase change of the metal from solid to liquid, does not change the general shape of the $ARS(\theta, \varphi)$ dependence significantly.

There are several differences between the experimental conditions and those used for the theoretical calculations. One of them is related to presence of multiple, rather than unique, surface defects (NPs), so multiple scattering between the different NPs may be important. It will be shown later that this factor does not play an important role in the processes studied. Another important difference is related to the size distribution function $S(d)$ of the studied NPs' ensemble. A very important feature of this distribution is its possible bimodal structure [10]. The function $S(d)$ depends strongly on the conditions of the NPs preparation and their material, showing the presence of not only a $S(d_b)$ maximum (at d_b equal to the mean NP size), but, very often, of an additional important maximum $S(d_s)$ for $d_s << d_b$ and $S(d_s) >> S(d_b)$ as well. As a result, small particles with small scattering cross-section can scatter the total amount of the SPP energy that is comparable to that scattered by large NPs.

The interrelations between $S(d_b)$ and $S(d_s)$ strongly depend on the conditions of the NPs preparation. The theoretical calculations of the space distribution of SPP scattering presented

#7080 - $15.00 US Received 5 April 2005; revised 16 May 2005; accepted 18 May 2005

above clearly show that variations of the defect size changes the angular position and width of the maximum of the scattered light. We found that for small NPs it is rather wide and directed backward, while for larger NPs, its intensity increases, and it becomes narrowly directed in the forward direction. So it is not surprising that there are two $ARS(\theta, \varphi)$ maxima that can be related to the corresponding maxima of the bimodal $S(d)$ distribution.

Moreover, the video-recording of the $I(\theta, \varphi, \iota)$ dependence clearly shows that, as the angle of incidence varies, both shapes and heights of these two maxima change in a different way, thus additionally confirming the above explanation.

The third distinction from the theoretical calculations is related to the difference in the shape of the defects: in our calculations, it was supposed they are either a protuberance or an indentation of Gaussian shape, while the experimentally analyzed NPs are truncated spheres. This is an important distinction; unfortunately we do not know of any published results for a half-sphere distribution of SPP scattering for spherical NPs. Another distinction is that in the experiments the Sn NPs are covered by the film of SiO_x, while no such film is present in the calculations. The next one is that the NPs are of a different metal than the substrate, while in the calculations the protuberances are of the same metal as the substrate. However, we believe that these differences do not change the qualitative behavior of our results.

Multiple scattering processes caused by the intrinsic prism, or the film interface roughness can be neglected because of its small rms values compared to the NP size and their high optical quality. However, due to the small distances between the NPs (comparable to their average size), multiple scattering process have to be taken into account when analyzing the effects produced by the surface roughness. Such processes are rather complicated, but for the current discussion can be approximately decomposed in the following way. The SPPs that are excited by the incident light can transfer their energy to: a) the air half-sphere of the scattered light. In this case, the plane of polarization of the scattered light keeps *P* orientation; b) another SPP with different direction of propagation in the surface plane. Its next scattering of the a) kind will give another direction of polarization for the scattered light in the air half-sphere whose orientation corresponds to the direction of propagation of the scattered SPP; c) light scattered into the prism half-sphere; c') part of c) that propagates oppositely to the incident light direction and participates in CBS processes; d) Joule losses.

Other SPPs can be as well scattered according to the above process, resulting in the next loop, and so on. According to this decomposition, a CBS experiment would give an estimation of the c') part of scattering, and one can state that it is negligibly small (see part 3.). One of the possible reasons is related to a small magnitude of the NP scattering cross-section. Another reason can be related to small efficiency of the transfer: incident light → SPPs → prism half-sphere of the scattered light.

The comparable values of the $ARS(\theta, \varphi, PS)$ distribution - Fig. 3(c), relative to the $ARS(\theta, \varphi, PP)$ distribution– Fig. 3(b) enables us to draw the conclusion that the b) → a) processes (incident light → multiple SPP → SPP scattering) are a very important contribution to the system studied in the present work.

5. Conclusion

The origin of one or two maxima in the $ARS(\theta, \varphi)$ dependence is related to the shape of the bimodal NP size distribution. The role of multiple light scattering in the processes studied is not so important, while the processes of multiple SPP scattering provide significant contributions to the observed $ARS(\theta, \varphi)$ distribution. A maximum in the angular dependence of the total integrated scatter appears for a much more extended range of effective surface roughness than the corresponding minimum in the specular reflectivity. Thus this well pronounced maximum can be used very effectively for monitoring surface optical parameters.

#7080 - $15.00 US Received 5 April 2005; revised 16 May 2005; accepted 18 May 2005

Acknowledgments

The authors are grateful to P. Cheyssac for his research contribution; they also highly appreciate fruitful discussions and collaboration with Prof. A.A. Maradudin. Partial support for this work from CNRS (French-Ukrainian collaboration project n°6987) is also appreciated.

#7080 - $15.00 US Received 5 April 2005; revised 16 May 2005; accepted 18 May 2005